Molecular Therapy
Nucleic Acids
Original Article

Overexpression of lncRNA EPB41L4A-AS1 Induces Metabolic Reprogramming in Trophoblast Cells and Placenta Tissue of Miscarriage

Yuanchang Zhu,[1,2,3,7] Qing Liu,[1,2,3,7] Meijian Liao,[1,2,3] Lianghui Diao,[4] Tonghua Wu,[4] Weijie Liao,[1,2] Ziqiang Wang,[1,2] Bing Li,[1,2] Shikuan Zhang,[1,3] Songmao Wang,[1,2] Weidong Xie,[2,3,5] Yuyang Jiang,[2] Naihan Xu,[2,3,5] Yong Zeng,[4] Burton B. Yang,[6] and Yaou Zhang[2,3,5]

[1]School of Life Sciences, Tsinghua University, Beijing 100084, P.R. China; [2]Key Lab in Healthy Science and Technology, Division of Life Science, Graduate School at Shenzhen, Tsinghua University, Shenzhen 518055, P.R. China; [3]State Key Laboratory of Chemical Oncogenomics, Graduate School at Shenzhen, Tsinghua University, Shenzhen 518055, P.R. China; [4]Shenzhen Key Laboratory for Reproductive Immunology of Preimplantation, Shenzhen Zhongshan Institute for Reproduction and Genetics, Fertility Center, Shenzhen Zhongshan Urology Hospital, Shenzhen 518055, P.R. China; [5]Open FIESTA Center, Tsinghua University, Shenzhen 518055, P.R. China; [6]Sunnybrook Research Institute and Department of Laboratory Medicine and Pathobiology, University of Toronto, Toronto, ON, Canada

Long non-coding RNAs (lncRNAs) have been shown to be crucial regulators in numerous human diseases. However, little is known about their effects on early recurrent miscarriage (RM). Here we aimed to investigate the role of lncRNA EPB41L4A-AS1 on placental trophoblast cell metabolic reprogramming, which might be involved in the pathogenesis of RM. After microarray and GEO database analyses, we found that EPB41L4A-AS1 was significantly increased in early RM placental tissue, and this increase may relate to estradiol-mediated upregulation of PGC-1α. EPB41L4A-AS1 overexpression inhibits glycolysis but increases the dependence on fatty acid oxidation in mitochondrion metabolism and suppresses the Warburg effect, which is necessary for rapid growth of the placental villus, leading to miscarriage. Mechanistic analyses demonstrated that EPB41L4A-AS1 functions as a lncRNA in the regulation of VDAC1 and HIF-1α expression through enhancement of H3K4me3 levels in the promoters of VDAC1 and HIF1A-AS1, a natural antisense transcript (NAT) lncRNA of HIF-1α. Taken together, these findings demonstrate that aberrant expression of EPB41L4A-AS1 is involved in the etiology of early RM, and it may be a candidate diagnostic hallmark and a potential therapeutic target for early RM treatment.

INTRODUCTION

Long non-coding RNAs (lncRNAs), usually more than 200 nt in length, are transcribed and processed in a similar manner as mRNA but often lack protein-coding potential.[1] Although lncRNAs are less well known compared with coding RNA and small non-coding RNAs, the number of new lncRNA has rapidly increased in recent years because more and more investigators are focused on this field. Strong evidence reports that lncRNAs participate in multiple cellular biological and pathological processes, including cell proliferation, cell death, and cell apoptosis;[2] cell senescence;[3] chromatin modification;[4,5] reprogramming of pluripotent stem cells;[6,7] genomic imprinting;[8] as well as initiation and progress of cancer cells.[9] Over the past few years, some studies have verified a clear correlation between lncRNAs and placental development, such as the lncRNAs HOTAIR,[10] HOXA11-AS,[11] and MEG3 and MALAT1,[12] and these lncRNAs appear to be involved in some pregnancy pathologies. However, the biological function of the lncRNA EPB41L4A-AS1 in early pregnancy placental tissue is completely unknown.

Studies have shown that lncRNAs might be involved in pregnancy pathologies, such as miscarriage.[13] Miscarriage, also called spontaneous abortion, can be defined as a pregnancy that terminates spontaneously before 20 weeks of gestation or a fetal weight of less than 500 g and affects 10%–15% of pregnant women.[14] It is one of the most common complications of early pregnancy.[15] About 1%–3% of pregnant women undergo two or more consecutive miscarriages, termed recurrent miscarriage (RM), and about 80% occur during the first trimester. Some specific factors, such as chromosome abnormalities,[16] thrombophilia,[17] endocrine disorders,[18] and infections,[19] can lead to miscarriage. Also, disruption of the immune tolerance system balance between the maternal-fetal interface is another significant cause of first-trimester miscarriage.[20,21] In addition, several investigations have shown that the risk of preeclampsia, fetal growth restriction, preterm birth, and stillbirth is significantly increased after

Received 19 November 2018; accepted 14 September 2019;
https://doi.org/10.1016/j.omtn.2019.09.017.

[7]These authors contributed equally to this work.

Correspondence: Yaou Zhang, Key Lab in Healthy Science and Technology, Division of Life Science, Graduate School at Shenzhen, Tsinghua University, Shenzhen 518055, P.R. China.
E-mail: zhangyo@sz.tsinghua.edu.cn
Correspondence: Burton B. Yang, Sunnybrook Research Institute and Department of Laboratory Medicine and Pathobiology, University of Toronto, Toronto, ON, Canada.
E-mail: byang@sri.utoronto.ca

a history of miscarriages.[22] More and more studies have verified that the metabolism of extravillous trophoblasts (EVTs) is impaired in miscarriage,[23] but there has only been a small number of reports regarding the participation of lncRNAs in EVT metabolism, such as glycolysis and fatty acid oxidative phosphorylation (OXPHOS).[24,25]

Recently, we reported that EPB41L4A-AS1 functions as an important regulator of metabolism reprogramming in tumor metabolism.[26] lnc EPB41L4A-AS1 is a lncRNA located in the 5q22.2 region of the genome, consisting of 3 exons that cover more than 3.5 kb in total DNA length (gene ID 114915). EPB41L4A-AS1 contains an 1,194-bp lncRNA gene in exon 1 that encodes a small outer mitochondrial membrane (OMM) protein, TIGA1 (transcript induced by growth arrest 1). Only a few papers have reported the function of EPB41L4A-AS1. Yabuta et al.[27] found that EPB41L4A-AS1 downregulation in tumors and its overexpression inhibit cell proliferation and cancer growth. In our recently published study, we reported that EPB41L4A-AS1 is a p53- and PGC-1α-regulated gene and that its downregulation in tumors triggers aerobic glycolysis, also known as the Warburg effect, to stimulate rapid tumor growth.[26] Like tumor cells, trophoblast cells are fast-growing cells and also need the Warburg effect to support their rapid growth.[28] Therefore, we wondered whether EPB41L4A-AS1 plays a role in placental growth by regulating the metabolism of trophoblast cells. Our hypothesis has been proven to be correct by the discoveries in this investigation, including a significant increase in EPB41L4A-AS1 expression in RM and inhibition of the Warburg effect in EPB41L4A-AS1 overexpression trophoblasts. Unraveling the role of EPB41L4A-AS1 will provide novel insights and a powerful therapeutic target for future treatment of early RM.

RESULTS

The Expression of EPB41L4A-AS1 Increases in Placental Tissue in Early RM

To identify the significant different transcription levels of lncRNAs in placental tissue between early RM (n = 3) and controls (n = 3), a lncRNA microarray analysis was performed. The results showed that 23 lncRNAs were significantly upregulated and 12 lncRNAs were downregulated in early RM placental tissue compared with the controls ($p < 0.05$), with EPB41L4A-AS1 being one of the markedly upregulated lncRNAs (Figure 1A). We further investigated the transcription levels of EPB41L4A-AS1 in several pregnancy pathologies from the GEO database. As shown in Figure 1B, the transcription level was significantly high in several common pregnancy pathologies, such as intrauterine growth restriction (IUGR; N = 36), preeclampsia (PE; N = 134), or miscarriage (N = 62), the differences reached statistical significance in the IUGR and PE groups compared with the controls (n = 103) ($p < 0.05$), especially the differences in the miscarriage group ($p < 0.01$). Next we determined the expression of EPB41L4A-AS1 in clinical specimens to confirm the microarray data and GEO database results. A total of 45 early RM patients and 23 artificial selective abortion patients were recruited to the study, with normal karyotypes after multiplex ligation-dependent probe (MLPA) examination. Baseline parameters were similar in the two groups (Table S2). The qRT-PCR results revealed that EPB41L4A-AS1 expression was significantly upregulated in early RM placental tissue ($p < 0.01$) (Figure 1C; Figure S1A). We further determined the expression of TIGA1 in early RM placental tissue and controls. TIGA1 is a small protein, located in the OMM and consisting of 120 amino acid residues, that is encoded by exon 1 in lncRNA EPB41L4A-AS1. Consistent with the results regarding the EPB41l4A-AS1 transcription level, TIGA1 protein levels were also significantly increased in placental tissue from early RM patients (Figure 1D). Immunohistochemical testing of placental tissue showed intense staining in the early RM group, and this difference was found to be statistically significant after quantitative analysis by PerkinElmer Vectra 2 (Figure 1E). Above all, these data showed that the expression of EPB41L4A-AS1 and its encoded protein was aberrantly high in miscarriage placental tissue and may be involved in the etiology of early RM.

Overexpression of EPB41L4A-AS1 in Placental Tissue May Be Related to Estradiol-Mediated Upregulation of PGC-1α

PGC-1α is a transcriptional coactivator that regulates mitochondrial biogenesis and energy metabolism through coactivation of key transcription factors, including estrogen-related receptor α (ERRα)[29] and nuclear respiratory factors (NRF-1 and NRF-2)[30] in multiple cell types. In our previous investigation, we reported that EPB41L4A-AS1 is a PGC-1α-regulated gene.[26] Here we further explored the relationship among EPB41L4A-AS1, PGC-1α, and ERRα or estrogen receptor α (ERα). The above data showed that EPB41L4A-AS1 expression was lower in placentas from normal pregnancies but significantly higher in pathological pregnancies, such as those with PE, IUGR, and early RM ($p < 0.05$). Furthermore, similar results emerged for the expression of PGC-1α, which was positively correlated with EPB41L4A-AS1 (Figure 2A; Figure S1B). In addition, protein expression was measured by western blotting of early RM placental tissue, and the results are presented in Figure 2B. PGC-1α was significantly expressed in early RM, consistent with the expression of PGC-1α mRNA. Therefore, we hypothesized that EPB41L4A-AS1 was regulated by PGC-1α. To determine whether PGC-1α is a transcription factor of EPB41L4A-AS1, we first examined the expression of PGC-1α and EPB41L4A-AS1 in early RM placental tissue using qRT-PCR, and a positive correlation was identified in clinical cases (Figure 2C; Figure S1C). To get a better understanding the biological role of EPB41L4A-AS1 in miscarriage placental tissue, we chose HTR8-S/Vneo (HTR8) cells as a model for the following studies. We knocked down PGC-1α in HTR8 cells and performed qRT-PCR and western blotting assays, which showed that knockdown of PGC-1α decreased EPB41L4A-AS1 expression and TIGA1 protein expression (Figures 2D and 2E). Conversely, both EPB41L4A-AS1 and TIGA1 expression was upregulated after transfection of HTR8 cells with PGC-1α and culture for 48 h (Figures 2F and 2G; Figure S1D). Subsequently, we explored whether PGC-1α regulated EPB41L4A-AS1 expression via binding of EPB41L4A-AS1 to its upstream region using a chromatin immunoprecipitation (ChIP) assay. The results demonstrated that PGC-1α regulated EPB41L4A-AS1 expression by binding to its promoter (Figure 2H).

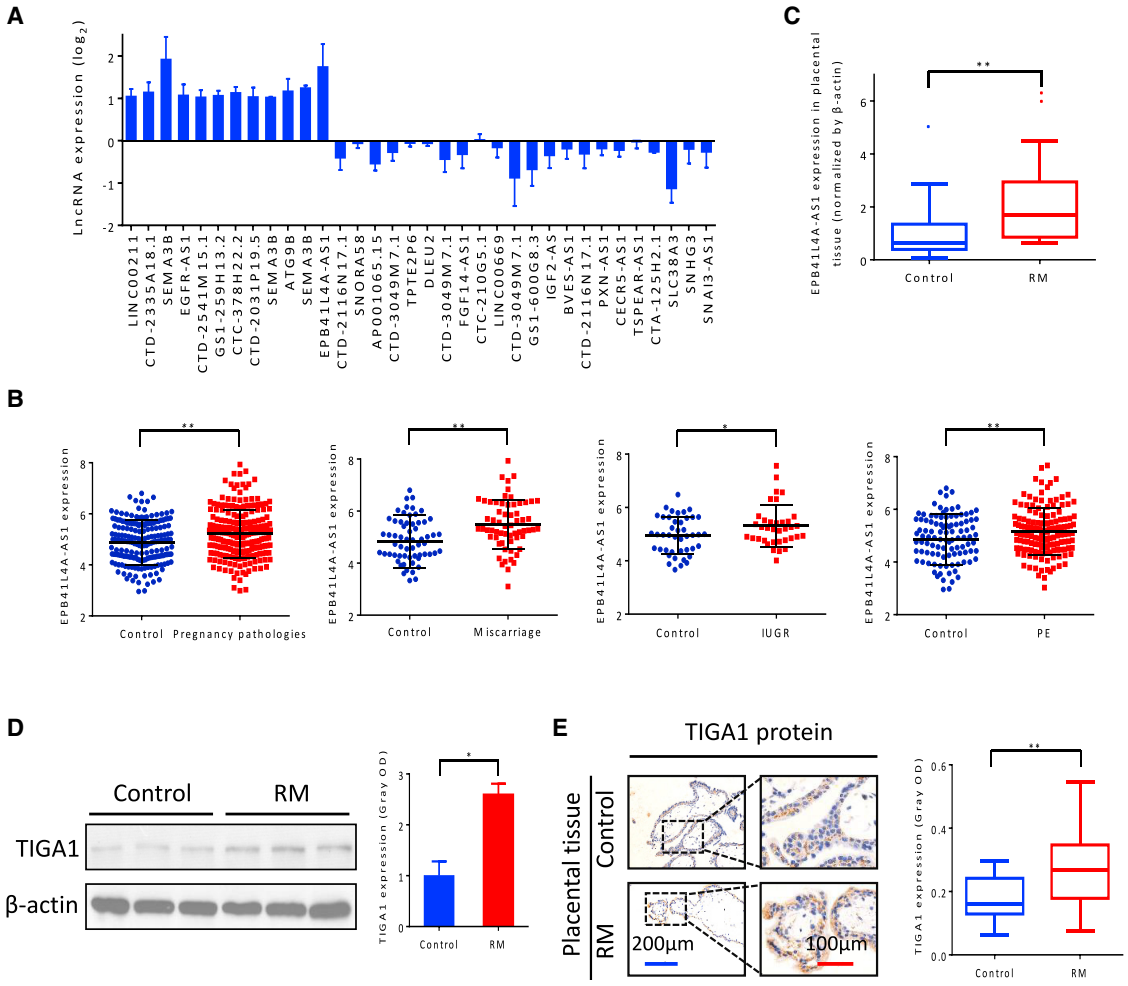

Figure 1. The Expression of EPB41L4A-AS1 Increases in Placental Tissue of Early RM

(A) Real-time PCR was used to determine the levels of significant differences in long non-coding RNAs in early RM placental trophoblast cells after lncRNA microarray (N = 3). EPB41L4A-AS1 was significantly higher in early RM groups ($p < 0.05$). (B) EPB41L4A-AS1 transcription levels were increased significantly in some pregnancy pathologies (N = 232) ($p < 0.01$) compared with normal placental tissue: early RM (N = 62, $p < 0.01$), IUGR (N = 36, $p < 0.05$), and PE (N = 144, $p < 0.05$). These data were collected from the GEO database. (C) The expression level of EPB41L4A-AS1 in our clinical sample was statistically higher in early RM placental tissue (N = 45) compared with the controls (N = 23), as shown by real-time PCR. (D) TIGA1 protein expression was increased dramatically in early RM placental tissue, as shown by western blot examination and quantitative analysis (N = 8) by ImageJ software. (E) Immunohistochemical staining of TIGA1 in early RM placental tissue. Quantitative analysis of TIGA1 intensity (N = 40) was performed using PerkinElmer Vectra 2. Stained TIGA1 was significant higher in the early RM group. Data are represented as means ± SD; *$p < 0.05$, **$p < 0.01$, Student's t test.

Estrogen-related receptor α (ERRα) can combine with PGC-1α to regulate both fatty acid oxidation and mitochondrial activity.[31] ERα has a gene structure highly homologous to ERRα, and estradiol levels were obviously increased during the first trimester. We then detected ERα expression and estradiol concentrations in RM patients. The results illustrated that estradiol concentrations in early RM blood plasma were raised significantly (Figure 2I), and ERα expression in human villous trophoblasts was increased dramatically compared with those in normal pregnancy(Figure 2J; Figure S1E). Further, PGC-1α and EPB41L4A-AS1 expression was activated following estradiol stimulation (Figures 2K and 2L; Figure S1F). Overall, *in vitro* and *in vivo* assays revealed that EPB41L4A-AS1 expression was regulated by PGC-1α and that estradiol may be involved in this regulation.

Overexpression of EPB41L4A-AS1 Induced Metabolic Reprogramming in Human Villous Trophoblasts

EPB41L4A-AS1 has been reported to be an important regulator of metabolism reprogramming in tumors, and we also found that it is dysregulated in miscarriage. Therefore, we wanted to determine the role of EPB41L4A-AS1 in early pregnancy and miscarriage. To elucidate gene expression levels in early RM placental tissue, a mRNA

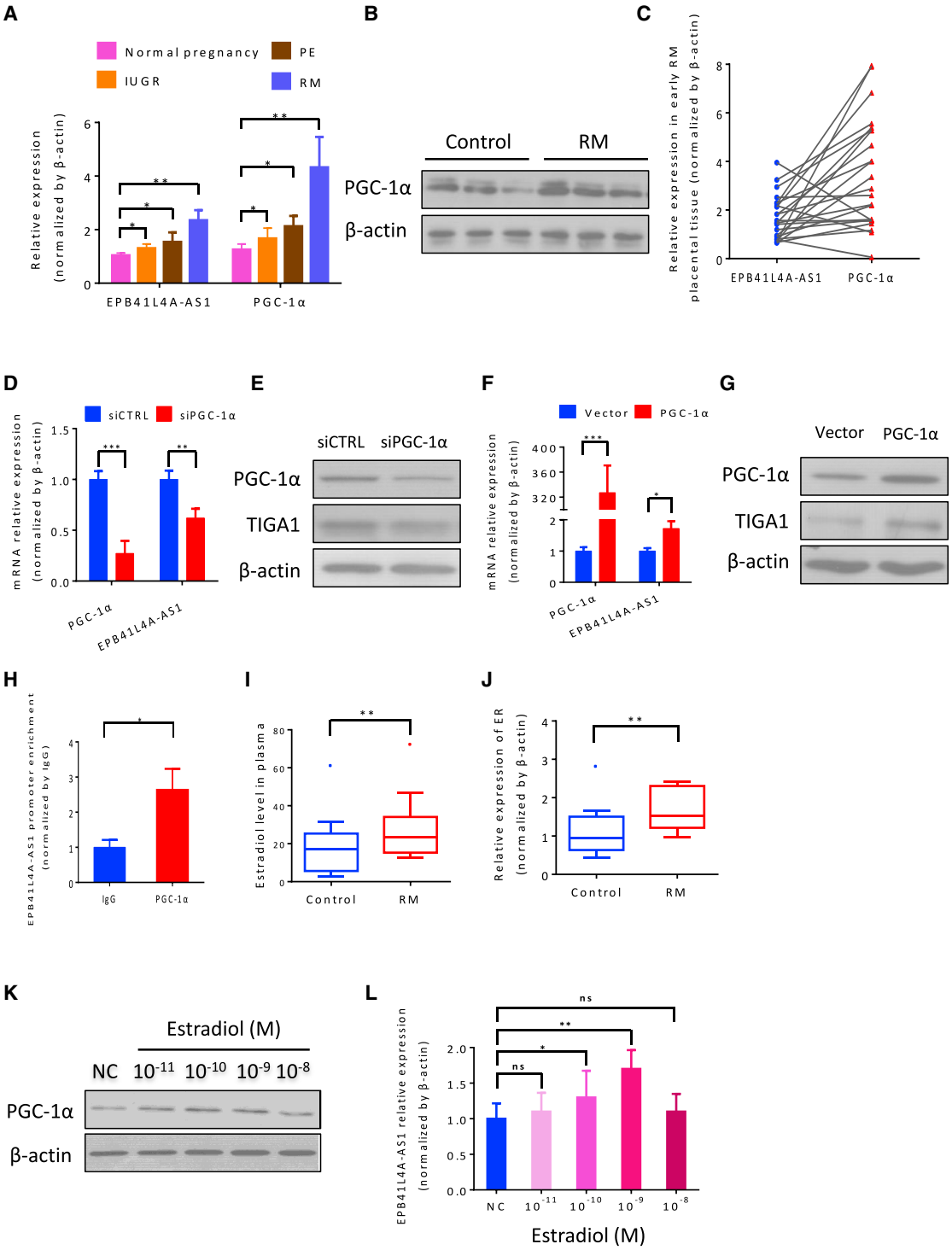

Figure 2. EPB41L4A-AS1 Expression Is Upregulated by PGC-1α

(A) The expression of EPB41L4A-AS1 and PGC-1α was higher in several pregnancy pathologies specimens, such as PE (N = 6), IUGR (N = 3), and RM (N = 6), compared with the control group (N = 6). (B) The protein expression of PGC-1α was dramatically higher in early RM placental tissue (N = 6, $p < 0.05$) compared with the controls (N = 6). (C) Positive correlation of PGC-1α mRNA and EPB41L4A-AS1 expression by qRT-PCR (N = 23). (D) EPB41L4A-AS1 and PGC-1α mRNA expression in HTR8 cells transferred

(legend continued on next page)

microarray analysis was performed. A total of 97 genes showed at least a 2-fold increase, whereas 294 genes showed significant decreases ($p < 0.05$). A clustering analysis showed that the expression of some genes related to glycolysis, such as HK2, HIF-1α, PKM, and PDK1, was increased significantly, whereas the expression of VDAC1, PGC-1α, and CPT1, which are related to OXPHOS, was increased significantly (Figure 3A). Then we classified the different genes using Kyoto Encyclopedia of Genes and Genomes (KEGG) analysis to obtain an overview of the signaling pathway distribution. The results showed that glycolysis, fatty acid metabolism, and the tricarboxylic acid (TCA) cycle were altered, suggesting that these pathways might be involved in the pathogenesis of early RM (Figure 3B). Moreover, a gene set enrichment analysis (GSEA) illustrated that high expression of EPB41L4A-AS1 inhibited glycolysis but enhanced mitochondrial activity; the genes annotated as part of the glycolytic cycle to glycolysis were remarkably enriched in the EPB41L4A-AS1 low expression group (Figure 3C). These data indicate that EPB41L4A-AS1 might participate in the initiation of early RM by inhibiting the glycolysis pathway and activating oxidative metabolism.

First we studied the effect of EPB41L4A-AS1 on glycolysis. HTR8 cells were transfected with EPB41L4A-AS1 small interfering RNA (siRNA) or an EPB41L4A-AS1 overexpression plasmid to obtain the downregulation or overexpression EPB41L4A-AS1 cell model, respectively (Figure S2A). We explored the effect of EPB41L4A-AS1 on glycolysis. The results of the extracellular acidification rate (ECAR) assay showed that glycolysis and glycolytic capacity displayed a 41% and 33% decrease after transfection with EPB41L4A-AS1 and culture for 48 h, respectively (Figures 3D and 3E). Conversely, EPB41L4A-AS1 knockdown caused increases in glycolysis, glycolytic capacity, and glycolytic reserve (36%, 30%, and 19% respectively), and the differences were statistically significant ($p < 0.05$) (Figures 3F and 3G). Next we examined the extracellular lactate concentration, which is the end product of glycolysis; it was approximately 13% decreased after EPB41L4A-AS1 overexpression and 38% increased after EPB41L4A-AS1 knockdown in lactate production ($p < 0.05$) (Figure 3H). Similar results were observed both in BeWo and JEG3 cells after EPB41L4A-AS1 knockdown and overexpression ($p < 0.05$) (Figures S2B, S2C, S2E, and S2F). Furthermore, several important enzymes involved in glycolysis, such as HIF-1α, HK2, and LDHA, were decreased by overexpression of EPB41L4A-AS1 ($p < 0.05$). On the contrary, the expression of these enzymes expression was increased following EPB41L4A-AS1 knockdown (Figure 3I). Similar changes mediated by EPB41L4A-AS1 knockdown and overexpression in BeWo and JEG3 cells were observed (Figures S2B–S2D). The above results demonstrated that glycolysis was blocked after EPB41L4A-AS1 overexpression in trophoblast cells and human villous trophoblasts.

EPB41L4A-AS1 overexpression not only downregulated glycolysis but also induced changes in mitochondrial function. Mitochondrial activation-related genes were significantly enriched in the EPB41L4A-AS1 high expression group after GSEA (Figure 3C). Cellular bioenergetics profile analysis using a Seahorse XFp analyzer demonstrated that EPB41L4A-AS1 overexpression in HTR8 cells led to an increase in mitochondrial basal respiration and proton leakage, and the difference between maximal respiration rate and spare respiratory capacity was statistically significant ($p < 0.05$) (Figures 4A and 4B). On the contrary, knockdown of EPB41L4A-AS1 resulted in a significant decrease in mitochondrial basal respiration, maximal respiration rate, and spare respiratory capacity ($p < 0.05$) (Figures 4C and 4D). However, ATP production was comparable in the EPB41L4A-AS1 overexpression and knockdown groups, and similar outcomes were found in both BeWo and JEG3 cells (Figure S3A). These results suggested that, even though OXPHOS was enhanced in the EPB41L4A-AS1 group, cellular energetics were not significantly increased. Furthermore, we detected several crucial genes involved in TCA cycle metabolism, such as VDAC1, PDK4, and PGC1α. The results showed that EPB41L4A-AS1 overexpression upregulated the expression of these genes, whereas their expression levels were significantly downregulated after EPB41L4A-AS1 knockdown; the data are shown in Figure 4E. Comparable findings were observed in BeWo cells and JEG3 cells (Figure S3B).

To our great interest, OXPHOS metabolism remained enhanced even though the glycolytic pathway was inhibited. Generally, there are three common pathways that promote OXPHOS: glucose oxidation, glutaminolysis, and fatty acid β-oxidation. In our study, glucose oxidation was suppressed because of a decrease in pyruvate formation, and transportation was blocked. Next, we needed to determine whether fatty acid oxidation and glutaminolysis metabolism affected the OXPHOS process. A mitochondrial fuel dependency assay showed that fatty acid oxidation was significantly enhanced by EPB41L4A-AS1 overexpression ($p < 0.05$), but EPB41L4A-AS1 knockdown resulted in a decrease in fatty acid respiration in HTR8 cells (Figure 4F). No significant changes were found in glutamate oxidation dependency in EPB41L4A-AS1 knockdown and overexpressed cells (Figure S3C). These results revealed that OXPHOS was raised by activation of the fatty acid β-oxidation pathway.

with siPGC-1α incubated for 48h. (E) TIGA1 and PGC-1α protein expression in HTR8 cell transferred with siPGC-1α incubated for 48h. (F) (EPB41L4A-AS1 and PGC-1α mRNA expression in HTR8 cells transferred with PGC-1α plasmid incubated for 48h. (G) TIGA1 and PGC-1α protein expression in HTR8 cell transferred with PGC-1α plasmid incubated for 48h. (H) The enrichment ofEPB41L4A-AS1 in the gene promoter regions was evaluated by ChIP-qPCR. IgG was used as negative control. (I) The estradiol concentration in RM plasma (N = 21) was higher compared with the controls, as shown by ELISA ($p < 0.05$), compared with the controls (N = 21). (J) The expression of EPB41L4A-AS1 was upregulated by different estradiol concentrations (10^{-11} to 10^{-8} M). (K) The expression of PGC-1α was detected by western blot after culture with different estradiol concentrations (10^{-11} to 10^{-8} M), and PGC-1α was significantly upregulated. (L) The relative expression of ER in RM placental tissue (N = 12) was examined by real-time PCR, and the results show that it was raised compared with the controls (N = 12). Data are represented as means SD; *$p < 0.05$, **$p < 0.01$, ***$p < 0.01$.

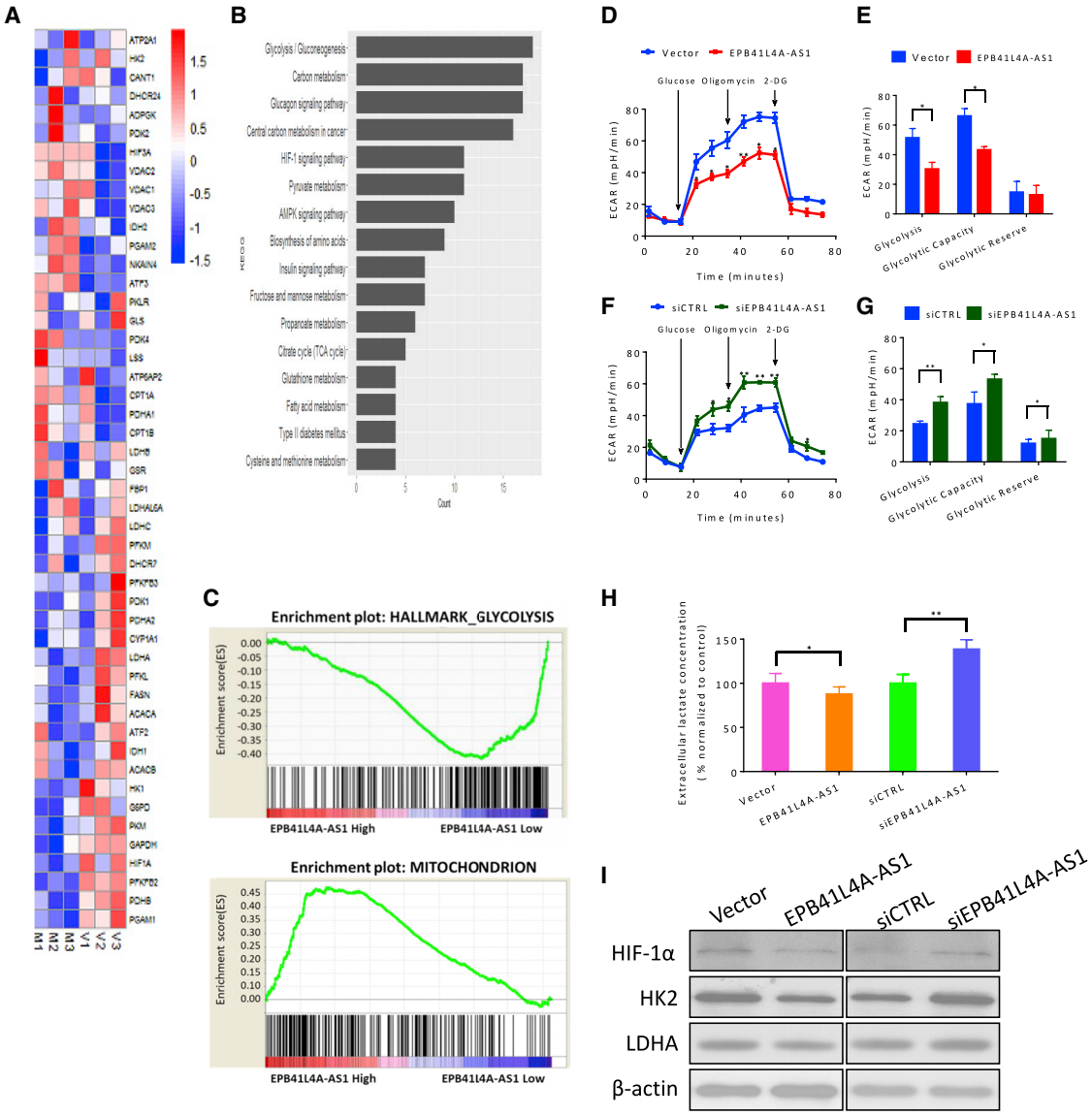

Figure 3. The Overexpression of EPB41L4A-AS1 Blocked the Glycolysis Process

(A) Glycolysis- and oxidative phosphorylation (OXPHOS)-related gene expression was analyzed by heatmap after mRNA microarray detection in early RM placental tissue (N = 3). (B) The metabolic process was analyzed by Kyoto Encyclopedia of Genes and Genomes (KEGG) for significantly different genes; some signaling pathways, such as glycolysis, HIF-1α signaling, and the TCA cycle, were different. (C) GSEA enrichment score curves show glycolysis related to low expression of EPB41L4A-AS1 but mitochondrial related to high expression of EPB41L4A-AS1 in 56 miscarriage cases compared with the controls (N = 56). (D) The Seahorse XFp assay detected the extracellular acidification rate (ECAR) in HTR8 cells with EPB41L4A-AS1 overexpression. (E) Quantification of glycolysis, glycolytic capacity, and glycolytic reserve after EPB41L4A-AS1 knockdown. Glycolysis and glycolytic capacity were significantly higher in the EPB41L4A-AS1 knockdown group ($p < 0.05$). Black arrows indicate the time point of cell treatment with different chemicals.(F) The Seahorse XFp assay detected the extracellular acidification rate (ECAR) in HTR8 cells with EPB41L4A-AS1 overexpression. (G) Quantification of glycolysis, glycolytic capacity, and glycolytic reserve after EPB41L4A-AS1 knockdown. Glycolysis and glycolytic capacity were significantly higher in the EPB41L4A-AS1 knockdown group ($p < 0.05$). (H) Extracellular lactate concentration was lower with EPB41L4A-AS1 overexpression but higher with EPB41L4A-AS1 knockdown in HTR8 cells ($p < 0.05$). (I) The expression of HIF-1α, HK2 and LDHA was decreased in the EPB41L4A-AS1 overexpression group but increased in the EPB41L4A-AS1 knockdown group in HTR8 cells. Data are represented as means ± SD. *$p < 0.05$, **$p < 0.01$, paired two-tailed Student's t test.

To further confirm the involvement of fatty acid oxidation in HTR8 cells, we found that carnitine, an important transporter of palmitic acid, was increased significantly after EPB41L4A-AS1 overexpression and decreased by EPB41L4A-AS1 knockdown (Figure 4G). In addition, fatty acid was examined 24 h and 48 h after transfection with EPB41L4A-AS1 siRNA or EPB41L4A-AS1 plasmid. Fatty acid

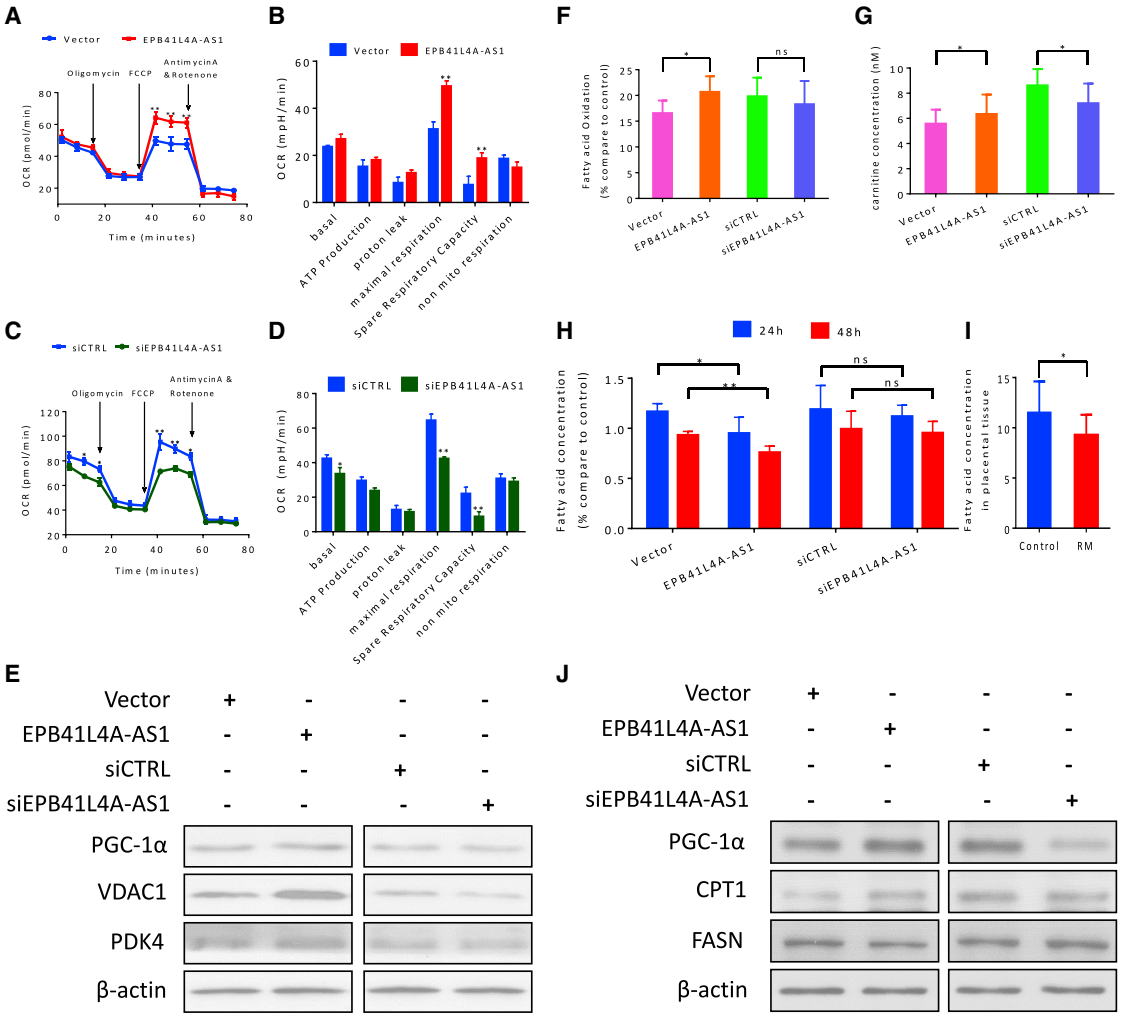

Figure 4. EPB41L4A-AS1 Overexpression Mediates Metabolic Reprogramming

(A) Seahorse XFp assays measured the oxygen consumption rate (OCR) in EPB41L4A-AS1 overexpression in HTR8 cells. (B) Basal respiration, ATP production, maximal respiration, spare respiratory capacity, proton leak, and non-mitochondrial respiration were increased in the EPB41L4A-AS1 overexpression group, and the difference reached statistical significance for maximal respiration ($p < 0.05$). (C) Seahorse XFp assays measured the oxygen consumption rate (OCR) in EPB41L4A-AS1 knockdown in HTR8 cells. Black arrows indicate the time points of cell treatment with different chemicals. The result showed that OCRs were significantly promoted in the EPB41L4A-AS1 overexpression group ($p < 0.05$). (D) Basal respiration, ATP production, maximal respiration, spare respiratory capacity, proton leak, and non-mitochondrial respiration were decreased in the EPB41L4A-AS1 siRNA group, and the difference reached statistical significance for maximal respiration ($p < 0.05$). (E) PGC-1α, VDAC1, and PDK4 expression was higher in HTR8 cells with EPB41L4A-AS1 overexpression but lower in HTR8 cells with EPB41L4A-AS1 knockdown. (F) Intracellular fatty acid oxidation was raised after EPB41L4A-AS1 overexpression, but there was no significant difference after EPB41L4A-AS1 knockdown in HTR8 cells. (G) The intracellular carnitine concentration was elevated after EPB41L4A-AS1 overexpression but decreased after EPB41L4A-AS1 knockdown in HTR8 cells. (H) The concentration of total fatty acid was detected by colorimetric assays in HTR8 cells after EPB41L4A-AS1 knockdown or overexpression with 24 h and 48 h. The fatty acid concentration was significantly decreased in the EPB41L4A-AS1 group both in cultured with 24 h and 48 h. (I) The intracellular fatty acid concentration was reduced in RM placental tissue. (J) The expression of oxidation-related enzymes (PDK4, VDAC1, and PGC-1α) were increased in the EPB41L4A-AS1 overexpression group but decreased in the EPB41L4A-AS1 knockdown group. All data are represented as means ± SD; *$p < 0.05$, **$p < 0.01$.

concentration was reduced significantly when EPB41L4A-AS1 was overexpressed at both cultured for 24 h and 48 h. No significant differences were found following EPB41L4A-AS1 knockdown at either 24 or 48 h (Figure 4H). The concentration of fatty acid was dramatically decreased in early RM placental tissues compared with controls (Figure 4I; Figures S3C and S3D).

Moreover, we examined several key enzymes that are crucial for fatty acid OXPHOS and synthesis, such as PGC1α, CPT1, and FASN. The results showed that PGC1α and CPT1 expression was increased, whereas FASN was inhibited by EPB41L4A-AS1 overexpression, suggesting that palmitic acid transportation and β-oxidation were enhanced, leading to accelerated fatty acid oxidation. The

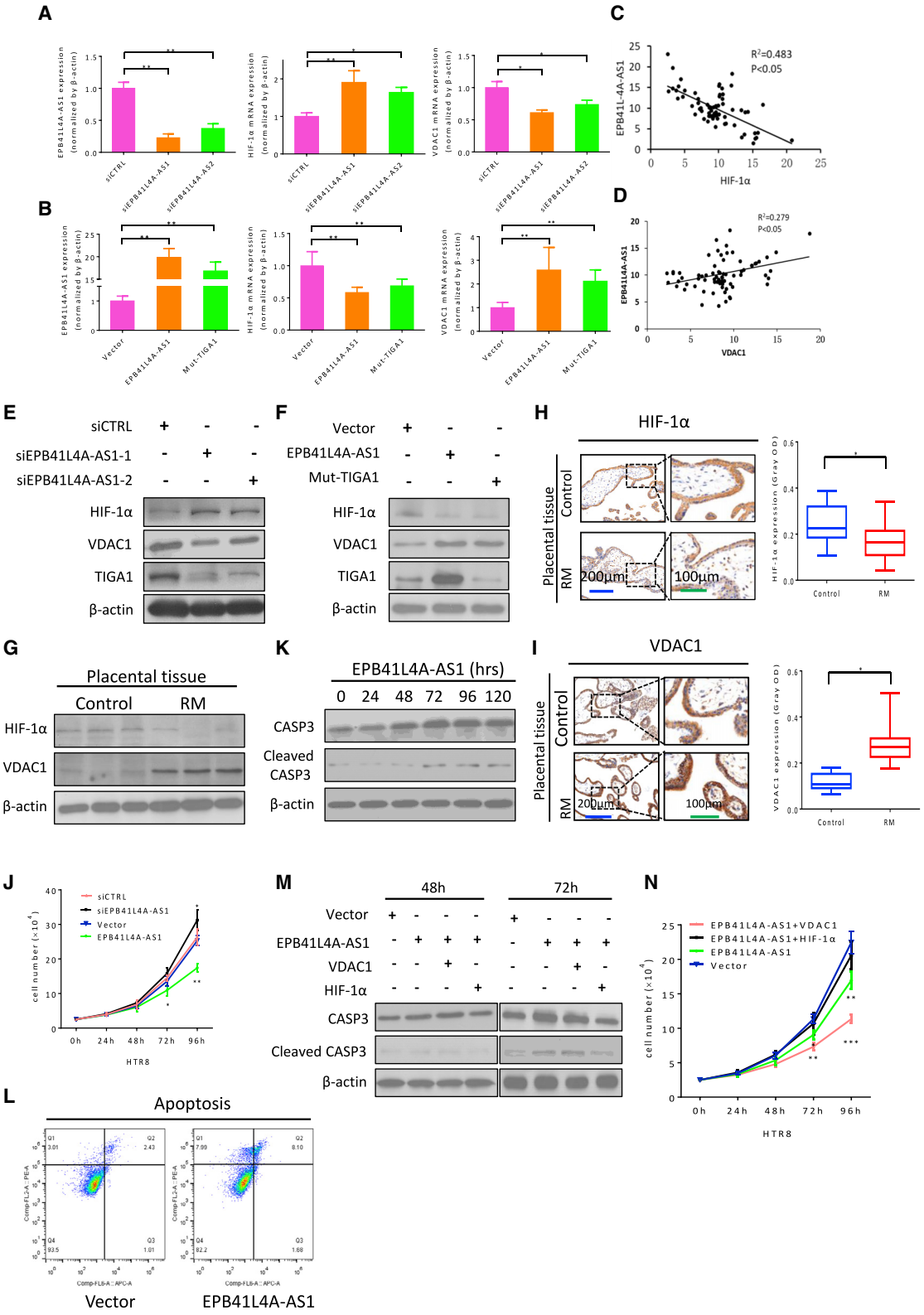

(legend on next page)

opposite effect was observed in EPB41L4A-AS1 knockdown cells (Figure 4J).

EPB41L4A-AS1 Functions as lncRNA to Regulate Cell Growth and Apoptosis via HIF-1α and VDAC1

Overexpression of EPB41L4A-AS1 caused metabolic disorder in human villous trophoblasts via dysregulation of metabolism-related genes. Among these genes, HIF-1α and VDAC1 play key roles in metabolic reprogramming. Because EPB41L4A-AS1 encodes a small OMM protein (13 kD), we first intended to find out whether the lncRNA EPB41L4A-AS1 itself or a protein derived from EPB41L4A-AS1 regulates the expression of VDAC1 and HIF-1α, two key metabolic genes. Therefore, the ATG mutated in a EPB41L4A-AS1 plasmid was constructed. The HIF-1α mRNA level was upregulated in HTR8 after transfection with two siEPB41L4A-AS1; however, it was downregulated after transfection with the EPB41L4A-AS1 plasmid, and a similar result was observed in the TIGA1 ATG mutation compared with the EPB41L4A-AS1 group. Correspondingly, VDAC1 mRNA expression was increased after transfection with EPB41L4A-AS1 and the EPB41L4A-AS1 ATG mutation, but it was reduced after EPB41L4A-AS1 knockdown (Figures 5A and 5B). Further, correlation analysis of clinical specimens demonstrated that VDAC1 has a positive relationship with the EPB41L4A-AS1 level but that HIF-1α has a negative relationship with EPB41L4A-AS1 expression (Figures 5C and 5D). In addition, we found that HIF-1α protein expression was increased but VDAC1 protein expression was decreased after EPB41L4A-AS1 knockdown (Figure 5E). Overexpression of EPB41L4A-AS1 inhibited HIF-1α and enhanced VDAC1 protein levels, whereas TIGA1 protein expression was totally blocked by the transfected TIGA1 ATG mutation; this did not affect HIF-1α and VDAC1 protein expression compared with the EPB41L4A-AS1 group (Figure 5F). Altogether, these data verified that EPB41L4A-AS1 is a lncRNA that regulates HIF-1α and VDAC1 expression. We also examined HIF-1α and VDAC1 expression in early RM placental tissue using western blotting and immunohistochemistry. The results showed that HIF-1α was significantly decreased whereas VDAC1 was dramatically increased in these tissues; more evidence suggesting that the metabolic pattern was disturbed in human villous trophoblasts (Figures 5G–5I).

The metabolic reprogramming caused by overexpression of EPB41L4A-AS1 inhibited the Warburg effect, which is necessary for rapid growth of the placental villus via downregulation of HIF-1α expression and upregulation of VDAC1. Furthermore, both HIF-1α and VDAC1 are apoptosis-related genes; therefore, we investigated the effect of EPB41L4A-AS1 on cell growth and apoptosis and whether it has an effect on cell proliferation and apoptosis. We observed the number of cells overexpressing EPB41L4A-AS1 following culture for several days. The results demonstrated that cell numbers were comparable within 48 h after transfection with the EPB41L4A-AS1 overexpression plasmid. However, the cell numbers were significantly decreased after culture for 72 h and 96 h ($p < 0.05$). In contrast, EPB41L4A-AS1 knockdown increased the cell number after incubation for 96 h (Figure 5J). Following, we found that total caspase-3 protein and cleaved caspase-3 protein were increased transfected with EPB41L4A-AS1 overexpression, and the difference was obvious after culture for 72 h (Figure 5K). Similar results were identified by flow cytometry after overexpression of EPB41L4A-AS1 for 72 h (Figure 5L). Moreover, cell apoptosis was aggravated after transfection with an EPB41L4A-AS1 plasmid, and apoptosis was worse when EPB41L4A-AS1 and VDAC1 plasmids were co-transfected, but it was reduced after co-transfection with EPB41L4A-AS1 and HIF-1α plasmids (Figure 5M). Cell numbers were decreased dramatically after transfection with EPB41L4A-AS1 and VDAC1 after culture for more than 72 h, but this was rescued after transfection with the HIF-1α plasmid as well (Figure 5N). These data show that metabolic reprogramming is mediated by overexpression of EPB41L4A-AS1, as demonstrated by suppression of the Warburg effect, inhibition of cell growth, and induction of apoptosis, which may be important causes of early RM.

EPB41L4A-AS1 Regulates VDAC1 Expression via Interaction with SET1A to Enhance H3K4me3 Levels in the VDAC1 Promoter

Histone modification is a common way by which lncRNAs regulate gene transcription. Therefore, we investigated the effect of

Figure 5. EPB41L4A-AS1 Is a lncRNA that Performs Biological Functions

(A) and (B) HIF-1α and VDAC1 gene expression was determined by qRT-PCR transfection with siEPB41L4A-AS1, the EPB41L4A-AS1 plasmid, or the EPB41L4A-AS1 ATG mutation plasmid. HIF-1α expression was increased in the EPB41L4A-AS1 knockdown group but decreased in the EPB41L4A-AS1 overexpression and EPB41L4A-AS1 ATG mutation groups; VDAC1 showed the opposite results. (C) Expression levels of VDAC1 mRNA and EPB41L4A-AS1 were positively correlated in early RM placental tissue (N = 73). (D) Expression levels of HIF-1α mRNA and EPB41L4A-AS1 were negatively correlated in early RM placental tissue (N = 73). (E) HIF-1α protein expression was higher but that of VDAC1 was lower in the EPB41L4A-AS knockdown group. (F) HIF-1α protein expression was downregulated in the EPB41L4A-AS1 and Mut-TIGA1 groups, but VDAC1 protein expression was upregulated in HTR8 cells. (G) HIF-1α protein expression was downregulated but VDAC1 was upregulated in RM placental tissue. (H) and (I) HIF-1α and VDAC1 protein expression was subjected to quantitative analysis by immunohistochemistry staining of RM placental tissue, and the difference reached statistical significance in the study group. (J) Cell numbers were calculated after EPB41L4A-AS1 overexpression or EPB41L4A-AS1 knockdown with different culture times (24, 48, 72, and 96 h). The cell numbers were reduced significantly in the EPB41L4A-AS1 group after culture for 72 h. (K) The expression of CASP3 and cleaved CASP3 was detected after EPB41L4A-AS1 overexpression with different culture times (24, 48, 72, and 96 h). Cell apoptosis was increased in the EPB41L4A-AS1 overexpression group after incubation for 72 h. (L) Cell apoptosis was raised by flow cytometer detection in the EPB41L4A-AS1 overexpression group. (M) The expression of CASP3 and cleaved CASP3 was increased after transfection with EPB41L4A-AS1, and this was aggravated by co-transfection with the VDAC1 plasmid but rescued after co-transfection with the HIF-1α plasmid with a different culture time. (N) The cell numbers were decreased after transfection with the EPB41L4A-AS1 and EPB41L4A-AS1+VDAC1 plasmids but rescued by the HIF-1α plasmid in the EPB41L4A-AS1 overexpression group within different culture times (24, 48, 72, and 96 h). Data are represented as means ± SD; *$p < 0.05$, **$p < 0.01$.

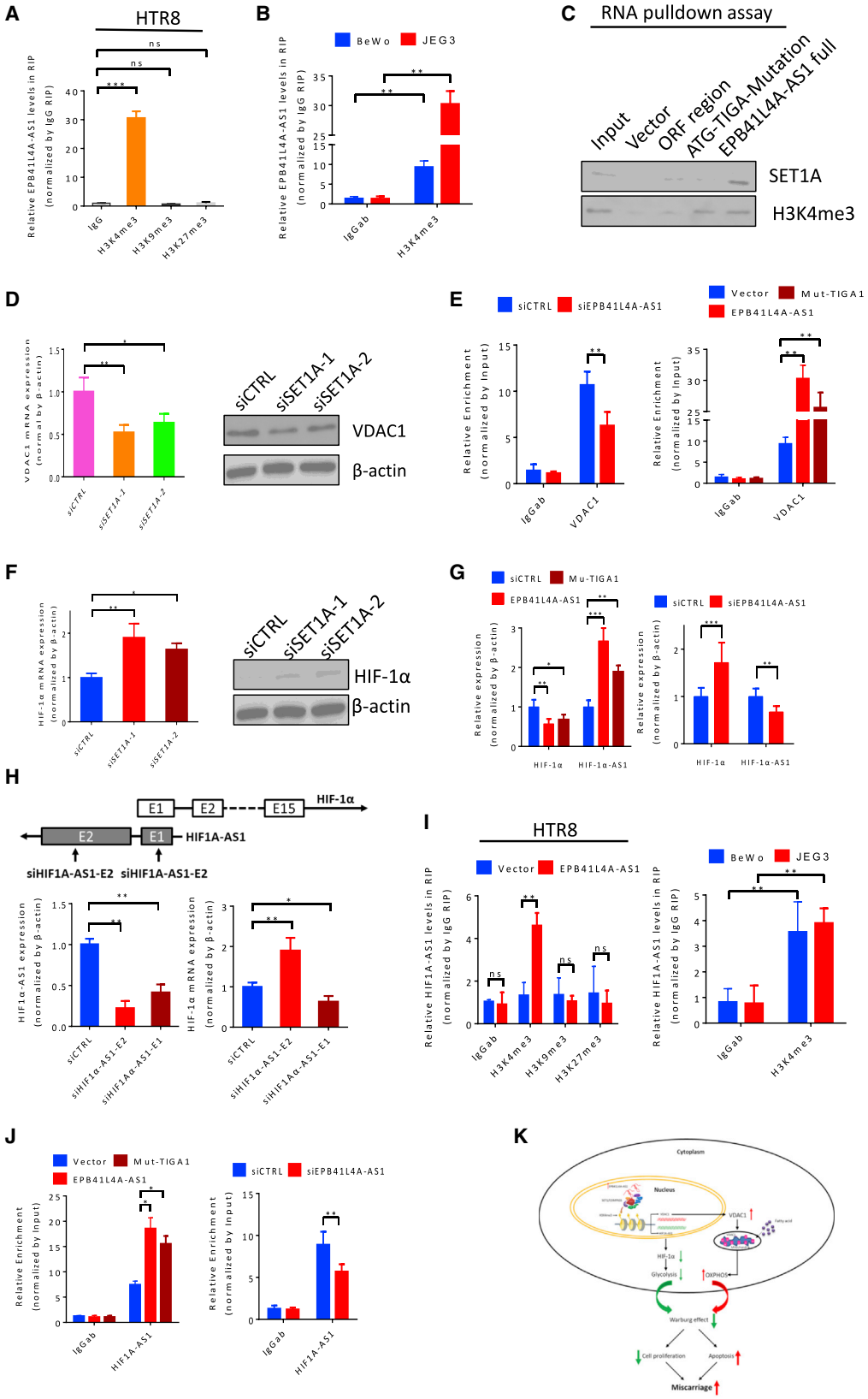

(legend on next page)

EPB41L4A-AS1 on histone modification of HIF-1α and VDAC1 promoters. RNA immunoprecipitation (RIP) assays were performed with H3K4me3, H3K9me3, and H3K27me3 antibodies. As shown in Figure 6A, H3K4me3 interacted with PB41L4A-AS1 in HTR8 cells. Comparable results were obtained in JEG3 and BeWo cells (Figure 6B). Furthermore, RNA pulldown assays also verified that EPB41L4A-AS1 interacted with H3K4me3 and SET1A (H3K4 trimethylation subunit composition) in HTR8 cells. The full-length RNA of the EPB41L4A-AS1, open reading frame (ORF) region with or without the ATG mutation were associated with H3K4me3 and SET1A, but the ORF region with or without the ATG mutation seemed to have a weaker interaction with H3K4me3 and SET1A (Figure 6C). These results demonstrated that the lncRNA EPB41L4A-AS1 could bind directly to SET1A. Next we blocked the expression of SET1A with siRNA and found that VDAC1 mRNA and protein levels were decreased significantly in HTR8 cells (Figure 6D). Then we hypothesized that EPB41L4A-AS1 may recruit SET1A to the VDAC1 promoter region, resulting in H3K4me3 enrichment in the VDAC1 region. Therefore, we performed ChIP assays to examine the enrichment of H3K4me3 in the promoter region of VDAC1. As shown in Figure 6E, silencing of EPB41L4A-AS1 suppressed VDAC1, and overexpression of EPB41L4A-AS1 increased VDAC1 enrichment. The TIGA1 ATG mutation presented similar results compared with the EPB41L4A-AS1 group.

EPB41L4A-AS1 Regulates HIF-1α Expression via HIF1A-AS1

If EPB41L4A-AS1 recruits more H3K4me3 to the promoter of the HIF-1α gene, then, in theory, expression of HIF-1α should increase. However, when we blocked SET1A expression with siRNA, the SET1A mRNA and protein levels were decreased significantly (Figure 6F). Confusingly, HIF-1α transcription and protein levels were decreased significantly (Figures 5A, 5E, and 5F). Knock out of EPB41L4A-AS1 promoted HIF-1α but inhibited HIF1A-AS1 expression; EPB41L4A-AS1 groups and TIGA1 ATG mutation were significantly enhanced HIF1A-AS1 expression but suppressed HIF-1α expression (Figure 6G). Further analysis found that HIF1A-AS1 and HIF-1α contain the same sequence in HIF-1α exon1, and we designed two siRNA, one applied in HIF1A-AS1 exon 1 and the other applied in HIF1A-AS1 exon 2. To confirm whether HIF-1α was regulated with HIF1A-AS1, we blocked HIF1A-AS1 expression by siHIF1A-AS1-E1 and siHIF1A-AS1-E2. The results showed that HIF1A-AS1 expression was downregulated by transfection with HIF1A-AS1 siRNA, and HIF-1α expression was significantly increased in the HIF1A-AS1-E2 group but decreased in the HIF1A-AS1-E1 group (Figure 6H), suggesting that HIF1A-AS1 regulates HIF-1α expression. To further examine whether HIF1A-AS1 was regulated by EPB41L4A-AS1, 3K4me3, H3K9me3, and H3K27me3 antibodies were used to perform a RIP assay. The results showed that EPB41L4A-AS1 only interacted with H3K4me3, and similar results were found in JEG3 and BeWo cells (Figure 6I). A ChIP assay was used to verify the enrichment of H3K4me3 in the promoter region of HIF1A-AS1. Overexpression of EPB41L4A-AS1 and the TIGA1 ATG mutation increased HIF1A-AS1 enrichment, but silencing of EPB41L4A-AS1 suppressed HIF1A-AS1 enrichment (Figure 6J).

DISCUSSION

Previous studies have evidenced that many lncRNAs have important roles in early pregnancy. lncRNAs such as MALAT-1 and HOXA11 have been verified to affect cell apoptosis, proliferation, migration, and invasion, resulting in abnormal pregnancy;[11,12] the lncRNA NEAT1 affects *corpus luteum* dysfunction, resulting in pregnancy failure.[32] Some lncRNAs are also involved in cell growth; EPB41L4A-AS2 and its encoded protein TIGA1 inhibit tumor proliferation and favorable prognoses in some cancers.[27,33] However, the function and biological significance of EPB41L4A-AS1 remain unclear, especially its role in early pregnancy. In our study, we found that EPB41L4A-AS1 shows an opposing expression trend in miscarriage compared with tumors. EPB41LA-AS1 expression is downregulated in many tumors, and this downregulation induces the Warburg effect, demonstrating an increase of glycolysis and glutamine dependence.[26] In RM, EPB41L4A-AS1 was dramatically upregulated in early RM placental tissue compared with normal pregnancy, and aberrant expression EPB41L4A-AS1 caused suppression of the Warburg effect in trophoblasts, demonstrating inhibition of glycolysis and increasing dependence on fatty acid oxidation. However, the

Figure 6. EPB41L4A-AS1 Recruits SET1A to Enhance the H3K4me3 Level in the VDAC1 Promoter and Regulates HIF-1α Expression via HIF1A-AS1

(A) RIP assays were performed using H3K4me3, H3K9me3, and H3K27Ac antibodies, and enrichment of EPB41L4A-AS1 was detected by qRT-PCR in HTR8 cells. EPB41L4A-AS1 was significantly enriched after incubation with H3K4me3 antibody ($p < 0.05$). (B) EPB41L4A-AS1 was enriched in JEG3 and BeWo cells after incubation with H3K4me3 antibody ($p < 0.05$). (C) The interaction of full-length EPB41L4A-AS1, the EPB41L4A-AS1 ATG mutation, and coding sequece region RNA with SET1A and H3K4me3 was evaluated by RNA pulldown assay. Full-length EPB41L4A-AS1 was combined with H3K4me3 antibody and the SET1A complex. (D) qRT-PCR and western blot assays showed that VDAC1 mRNA and protein expression was downregulated after SET1A knockdown in HTR8 cells. (E) The enrichment of H3K4me3 in the promoter regions of VDAC1 were increased via ChIP assays after transfection with the EPB41L4A-AS1 plasmid and the EPB41L4A-AS1 ATG mutation plasmid in HTR8 cells but decreased in the EPB41L4A-AS1 knockdown group. (F) HIF-1α gene and protein expression was elevated after SET1A knockdown in HTR8 cells, which was examined by qRT-PCR and western blot assays. (G) HIF-1α was increased in the EPB41l4A-AS1 knockdown group and decreased in the EPB41L4A-AS1 and EPB41L4A-AS1 ATG mutation groups in HTR8 cells. HIF1A-AS1 showed the opposite result. (H) Structure chart of HIF-1α and HIF1A-AS1.The expression of HIF-1α was increased in SET1A siRNA1 but decreased in SET1A siRNA2. (I) The enrichment of HIF1A-AS1 was detected by qRT-PCR in HTR8/BeWo/JEG3 cells after treatment with H3K4me3, H3K9me3, and H3K27Ac antibodies using RIP assays. HIF1A-AS1 was significantly enriched after incubation with H3K4me3 antibody, and similar results were found for BeWo and JEG3 cells. (J) The enrichment of HIF1A-AS1 was identified via ChIP assays after transfection with siEPB41l4A-AS1, EPB41L4A-AS1, or EPB41L4A-AS1 ATG mutation in HTR8 cells. HIF1A-AS1 was increased in the EPB41L4A-AS1 and EPB41L4A-AS1 ATG mutation groups and decreased in the EPB41L4A-AS1 knockdown group. (K) Schematic model of mediation by EPB41L4AAS1 in shifting the metabolic reprogramming of early RM. Data are represented as means ± SD; *$p < 0.05$, **$p < 0.01$, unpaired two-tailed Student's t test.

metabolic reprogramming mediated by EPB41L4A-AS1 dysregulation in both tumor and miscarriage seems to occur through the HIF-1α and VDAC1 signaling pathways. It is well known that placental tissue displays a phenotype strikingly like cancer cells, which prefer to use glycolysis to maintain rapid cell proliferation and differentiation without oxidative stress.[34,35] The Warburg effect is necessary for rapid growth of the placental villus. Metabolic reprogramming mediated by EPB41L4A-AS1 overexpression not only decreased cell growth via inhibition of the Warburg effect but also induced apoptosis in placental trophoblasts through dysregulation of VDAC1 and HIF-1α, eventually resulting in early miscarriage (Figure 6K).

As we know, VDAC1 is an important cellular metabolite transporter in mitochondria, and one of its main functions is to mediate the exchange of metabolites, such as pyruvate, malate, succinate, glutamate citrate, and NADH, between the cytosol and mitochondria.[36,37] VDAC1 also participates in the regulation of mitochondrion-mediated apoptosis by binding with Bax to exert proapoptotic activity.[38] However, hexokinases (HKs) can compete with Bax for binding to VDAC1, reducing its proapoptotic activity.[39] In this investigation, EPB41L4A-AS1 enhanced VDAC1 expression by recruitment of the SET1A/COMPASS complex to the VDAC1 promoter and increasing H3K4me3 levels of VDAC1. On the other hand, EPB41L4A-AS1 overexpression downregulated HIF-1α expression, which caused a decrease in HK2 levels. Increased VDAC1 and decreased of HK2 may result in apoptosis. In our previous study, we found that VDAC1 closure or reduction not only decreases metabolite exchange but also increases oxidative stress in mitochondria through the P-eIF2α pathway, finally enhanced reactive oxygen species, and accumulation of HIF-1α.[26]

Although VDAC1 is a crucial gene for cell metabolism, HIF-1α is another key multifunctional factor and a central regulator of glycolysis, especially in hypoxia.[40,41] Numerous studies have reported that HIF-1α and its accumulation appeared to play a crucial role in glycolysis activity.[42–45] In our study, we found that overexpression of EPB41L4A-AS1 decreased HIF-1α expression by enhancing expression of HIF1A-AS1, an antisense lncRNA for HIF-1α. We found that HIF1A-AS1 inhibits HIF-1α expression mainly through a natural antisense transcription mechanism.[46]

It is well known that many lncRNAs are located in the cell nucleus and regulate gene expression mainly via histone modification. In recent years, several studies have reported that some of lncRNAs encode a small protein or peptides to partly perform their biological functions.[11,45] EPB41L4A-AS1 was first reported to encode a small mitochondrial located protein, TIGA1; aberrantly high expression of TIAG1 suppresses tumor cell proliferation.[27] In our study, we found that both EPB41L4A-AS1 and TIGA1 had significantly high expression in early RM placental tissue. However, it is unknown whether EPB41L4A-AS1 or TIGA1 perform biological functions; this is an important concern in the study. TIGA1 with a mutated ATG was placed on a plasmid and transfected into HTR8 cells. After transfection with the ATG-TIGA1 mutation, the TIGA1 protein was totally inhibited, whereas the proteins of HIF-1α and VDAC1 were not markedly affected. Correspondingly, HIF-1α and VDAC1 gene expression was altered significantly compared with the EPB41L4A-AS1 group. Furthermore, an RNA pulldown assay showed that the ATG-TIGA1 mutation could recruit and bind to a histone methylation modification complex, including SET1A in the nucleus, to regulate gene expression. Moreover, the VDAC1 gene promoter was enriched in the ATG-TIGA1 mutation compared with the vector group but closed to EPB41L4A-AS1 group. A ChIP assay illustrated that the ATG-TIGA1 mutation had a similar function as EPB41L4A-AS1, regulating VDAC1 gene expression by binding to its promoters. Taken together, our results show that EPB41L4A-AS1 is mainly a lncRNA, not a protein performing biological functions.

Given the above, we explored a key role of EPB41L4A-AS1 in blocking glycolysis and enhancing dependence on fatty acid oxidation, resulting in metabolic reprogramming because of regulation of HIF-1α and VDAC1 expression, finally affecting placental proliferation and promoting cell apoptosis. Therefore, EPB41L4A-AS1 may be an early diagnostic hallmark candidate and, in the future, might become a powerful therapeutic target for unexplained early miscarriage.

MATERIALS AND METHODS

Total DNA/RNA Extraction and Purification

From June 2015 to December 2016, a total of 113 placental chronic villous samples were obtained from early recurrent miscarriage patients who came to the fertility center of Shenzhen Zhongshan Urology Hospital within gestational age 6–10 weeks after assisted reproductive technique treatment because of termination of embryonic development. 27 patients' placental tissues were used in the control groups with artificial selective abortion for personal reasons and no history of recurrent miscarriage; the gestational age was similar between the two groups (Table S2). After curettage, the placental tissue was transported to the laboratory within 30 min.

After dissecting the tissue, total RNA was extracted using the miRNeasy Mini Kit (QIAGEN, Germany, 217004), and DNA was isolated using the DNeasy Blood and Tissue kit (QIAGEN, Germany, 69506) according to the manufacturer's methods. High-quality RNA was acquired by RNase-Free DNase digestion and then dissolved in elution buffer. The purity, concentration, and quantification of all DNA and RNA samples were assessed using a Nanodrop spectrophotometer (Shimadzu, Japan) and then stored at −20°C for preparation or for the next experiment. This study was approved by the Research Ethics Committee of Shenzhen Zhongshan Urology Hospital, and all women provided informed consent prior to the study.

lncRNA and mRNA Microarray Analysis

Chromosome copy number variations were detected by multiplex ligation-dependent probe methods with the SALSA P036 and P181 Probe Mix Kits (MRC-Holland, the Netherlands) to exclude whole or segmental chromosome aneuploidy. The lncRNA and mRNA

microarrays were examined using the human whole-genome 4 × 44K array (CapitalBio Tech, China) containing approximately 35,000 human transcripts with cRNA probes at the core facility of GenoCheck. The significantly different transcription levels of mRNA and lncRNA were evaluated by the ratio (>2 or <0.5) of RNA expression in unexplained early RM compared with the control groups.

Bioinformatics Analysis

Microarray analysis of gene expression was performed using the Affymetrix platform. Basic bioinformatics analyses of data, including normalization, annotations, experimental group comparisons with fold change, and p value calculations, were performed at the Bioinformatics and Gene Expression Analysis (BGEA) core facility of the Karolinska Institutet. Gene Ontology (GO; http://geneontology.org/) terms and KEGG (https://www.genome.jp/kegg/) pathways were analyzed for significant differences of metabolism-related genes. Pregnancy pathology data were downloaded from the GEO database (https://www.ncbi.nlm.nih.gov/geo/). GSEA (http://software.broadinstitute.org/gsea/index.jsp) was performed using GSEA 2-2.2.2 software. Expression correlation between EPB41L4A-AS1 and PGC-1α or HIF-1α or VDAC1 in trophoblast cell was examined by Spearman correlation test.

Cell Culture and Real-Time PCR

HTR8 cells were donated by Prof. Haixiang Sun (Nanjing Drum Tower Hospital), and BeWo and JEG3 cells were purchased from the ATCC. Cells were cultured in RPMI 1640 medium (containing 10% FBS, 10 units/mL penicillin, and 10 mg/mL streptomycin) in 5% CO_2 at 37°C. For EPB41L4A-AS1 gene overexpression or knockdown, 1 μg plasmids or 50 nM siRNA were transfected using Lipofectamine 3000 (Invitrogen, 1656200) as described by the manufacturer.

A total of 500 ng RNA was subjected to reverse transcription using the M-MLV reverse transcriptase kit (Toyobo, Japan) for cDNA synthesis. Gene reverse transcription used ReverTra Ace Master Mix (Toyobo, FSQ-301), and mRNA expression was tested using an ABI7500 cycler (USA) with the SYBR Green PCR kit (Toyobo, Hilden, Japan) and normalizing to β-actin mRNA. All primer sequences are listed in Table S1. All PCRs were performed in triplicate.

Protein Expression Analysis

Protein extracts were prepared in RIPA lysis buffer (50 mM Tris-HCl [pH 7.4], 180 mM NaCl, 1% Triton X-100, 15% glycerol, and 1 mM EDTA) supplemented with 1 mM DTT and 0.5 mM PMSF. Protein extracts were resolved with SDS-PAGE and transferred into nitrocellulose (NC) membranes. They were then blocked with 5% BSA in TBST buffer within 30 min and incubated for 1–2 h with the following primary antibodies: TIGA1 (Proteintech, 24698-1-AP), β-actin (Proteintech, 60008), VDAC1 (Novus Biologicals, NBP100-695), PGC-1α (Cell Signaling Technology, 5536), LDHA (Cell Signaling Technology, 3582), HIF-1α (Abcam, ab1), HK2 (Cell Signaling Technology, 2867), FASN (Cell Signaling Technology, 3180), PDK4 (Novus Biologicals, NBP1-54723), and CPT1 (Cell Signaling Technology, 12252). Then NC membranes were incubated with horseradish peroxidase-coupled specific secondary antibodies for 1 h. Finally, these protein bands were visualized with ECL blotting detection reagents (KPL, 547100), and gray values were calculated with ImageJ software.

Mitochondrial Respiration and Glycolysis Measurements

Glycolysis and mitochondrial respiration rates were measured in an XF96 extracellular flux analyzer (Seahorse Bioscience, Agilent, USA). XF base medium was added to 2 mM glutamine, and the pH level was to 7.4 with 0.1 N NaOH at 37°C before the next assay. Approximately 8,000–10,000 cells per well were cultured in XFp 8-well microplates and incubated overnight. The following day, cells were harvested and detected using the Glycolysis Stress Test Kit (Invitrogen, part number 103017-100), Cell Mito Stress Test Kit (Invitrogen, part number 103010-100), and XF Mito Fuel Flex Test Kit (Invitrogen, part number 103270-100) according to the manufacturer's protocols.

Flow Cytometry and Colorimetric Assays

Cells were subjected to EPB41L4A-AS1 overexpression and knockdown, cultured for 48 h, harvested, incubated in NADPH antibody for 1 h, washed with PBS, resuspended in growth medium, and immediately analyzed by flow cytometry (absorption spectrum [abs.] 488 nm/em. 562 nm). The total cellular LDHA in the medium supernatant (Biovision, K607-100) and ATP (Biovision, K354-100) concentration were determined by colorimetric assay.

CHIP Assay

HTR8 cells were fixed using 1% formaldehyde and harvested on ice with ChIP lysis buffer (50 mM Tris-HCl [pH 8.0], 5 mM EDTA, 0.1% deoxycholate, 1% Triton X-100, 150 mM NaCl, and proteinase inhibitor) after transfer of the EPB41L4A-AS1 siRNA and overexpression plasmid and culture for 48 h. Subsequently, the cells were sonicated, and the supernatant was collected and incubated with Dynabeads protein G and primary antibody (H3K4me3, Cell Signaling Technology, 9751). After incubation for 2 h, the complex was washed three times, and DNA was purified and condensed. Finally, the DNA fraction was analyzed by real-time PCR.

RNA Pulldown Assay

Different fractions of EPB41L4A-AS1 were constructed with the pcDNA3.1 plasmid containing the T7 promoter. The RNA pulldown assay was performed following the protocol of the Pierce Magnetic RNA-Protein Pull-Down Kit (Thermo Fisher Scientific, USA). Antibodies, including SET1A and H3K4me3, were purchased from Cell Signaling Technology.

RNA Immunoprecipitation Assay

Cells were harvested and lysed with polysome lysis and then incubated with 2 μg H3K4me3, H3K9me3, and H3K27Ac antibodies overnight at 4°C. Then they were washed and incubated with Dynabeads protein A for about 4 h at 4°C. We washed and precipitated the RNA with ethanol and sodium acetate, and then the extracted RNA was reverse transcribed and detected by qRT-PCR.

Data Analysis

The results are presented as the mean ± SD; data plotting was performed by Prism Graph Pad 6.0 and statistical analysis by SPSS 22.0. $p < 0.05$ and $p < 0.01$ were considered statistically significant. Unpaired, two-tailed Student's t test, ANOVA, Z test, log-rank test, or Mann-Whitney test was used to compare the results between two groups. Each experiment was repeated three times.

SUPPLEMENTAL INFORMATION

Supplemental Information can be found online at https://doi.org/10.1016/j.omtn.2019.09.017.

AUTHOR CONTRIBUTIONS

Burton, Yaou Zhang: supervised and supported the study. Yuanchang Zhu, Qing Liu: designed and wrote the manuscript write. Bing Li, Ziqiang Wang, Meijian Liao: bioinformatics analysis. Weidong Xie, Naihan Xu and Yuyang Jiang: date collection. Tonghua Wu: real-time PCR assay. All authors read and approved the final manuscript.

CONFLICTS OF INTEREST

The authors declare no competing interests.

ACKNOWLEDGMENTS

This work was supported by the National Natural Science Foundation of China (31571400), the Basic Research Fund of Shenzhen (JCYJ20170405103953336), Special Project of Suzhou-Tsinghua Innovation Leading Action (2016SZ3012), and specific funding from the Clinical Medical Research of Chinese Medical Association—Reproductive Medicine Clinical Research and Development Youth Program (18010130742).

REFERENCES

1. Djebali, S., Davis, C.A., Merkel, A., Dobin, A., Lassmann, T., Mortazavi, A., Tanzer, A., Lagarde, J., Lin, W., Schlesinger, F., et al. (2012). Landscape of transcription in human cells. Nature *489*, 101–108.
2. Sun, M., Nie, F., Wang, Y., Zhang, Z., Hou, J., He, D., Xie, M., Xu, L., De, W., Wang, Z., and Wang, J. (2016). LncRNA HOXA11-AS Promotes Proliferation and Invasion of Gastric Cancer by Scaffolding the Chromatin Modification Factors PRC2, LSD1, and DNMT1. Cancer Res. *76*, 6299–6310.
3. Bassett, A.R., Akhtar, A., Barlow, D.P., Bird, A.P., Brockdorff, N., Duboule, D., Ephrussi, A., Ferguson-Smith, A.C., Gingeras, T.R., Haerty, W., et al. (2014). Considerations when investigating lncRNA function in vivo. eLife *3*, e03058.
4. Alcid, E.A., and Tsukiyama, T. (2014). ATP-dependent chromatin remodeling shapes the long noncoding RNA landscape. Genes Dev. *28*, 2348–2360.
5. Huang, Y., Jin, C., Zheng, Y., Li, X., Zhang, S., Zhang, Y., Jia, L., and Li, W. (2017). Knockdown of lncRNA MIR31HG inhibits adipocyte differentiation of human adipose-derived stem cells via histone modification of FABP4. Sci. Rep. *7*, 8080.
6. Yin, Y., Yan, P., Lu, J., Song, G., Zhu, Y., Li, Z., Zhao, Y., Shen, B., Huang, X., Zhu, H., et al. (2015). Opposing Roles for the lncRNA Haunt and Its Genomic Locus in Regulating HOXA Gene Activation during Embryonic Stem Cell Differentiation. Cell Stem Cell *16*, 504–516.
7. Liu, J., Li, Y., Lin, B., Sheng, Y., and Yang, L. (2017). HBL1 Is a Human Long Noncoding RNA that Modulates Cardiomyocyte Development from Pluripotent Stem Cells by Counteracting MIR1. Dev. Cell *42*, 333–348.e5.
8. Latos, P.A., Pauler, F.M., Koerner, M.V., Şenergin, H.B., Hudson, Q.J., Stocsits, R.R., Allhoff, W., Stricker, S.H., Klement, R.M., Warczok, K.E., et al. (2012). Airn transcriptional overlap, but not its lncRNA products, induces imprinted Igf2r silencing. Science *338*, 1469–1472.
9. Kogo, R., Shimamura, T., Mimori, K., Kawahara, K., Imoto, S., Sudo, T., Tanaka, F., Shibata, K., Suzuki, A., Komune, S., et al. (2011). Long noncoding RNA HOTAIR regulates polycomb-dependent chromatin modification and is associated with poor prognosis in colorectal cancers. Cancer Res. *71*, 6320–6326.
10. Zhang, Y., Jin, F., Li, X.C., Shen, F.J., Ma, X.L., Wu, F., Zhang, S.M., Zeng, W.H., Liu, X.R., Fan, J.X., et al. (2017). The YY1-HOTAIR-MMP2 Signaling Axis Controls Trophoblast Invasion at the Maternal-Fetal Interface. Mol. Ther. *25*, 2394–2403.
11. Xu, Y., Wu, D., Liu, J., Huang, S., Zuo, Q., Xia, X., Jiang, Y., Wang, S., Chen, Y., Wang, T., and Sun, L. (2018). Downregulated lncRNA HOXA11-AS Affects Trophoblast Cell Proliferation and Migration by Regulating RND3 and HOXA7 Expression in PE. Mol. Ther. Nucleic Acids *12*, 195–206.
12. Chen, H., Meng, T., Liu, X., Sun, M., Tong, C., Liu, J., Wang, H., and Du, J. (2015). Long non-coding RNA MALAT-1 is downregulated in preeclampsia and regulates proliferation, apoptosis, migration and invasion of JEG-3 trophoblast cells. Int. J. Clin. Exp. Pathol. *8*, 12718–12727.
13. Liu, L.P., and Gong, Y.B. (2018). LncRNA-TCL6 promotes early abortion and inhibits placenta implantation via the EGFR pathway. Eur. Rev. Med. Pharmacol. Sci. *22*, 7105–7112.
14. Popescu, F., Jaslow, C.R., and Kutteh, W.H. (2018). Recurrent pregnancy loss evaluation combined with 24-chromosome microarray of miscarriage tissue provides a probable or definite cause of pregnancy loss in over 90% of patients. Hum. Reprod. *33*, 579–587.
15. Kavalier, F. (2005). Investigation of recurrent miscarriages. BMJ *331*, 121–122.
16. Elghezal, H., Hidar, S., Mougou, S., Khairi, H., and Saâd, A. (2007). Prevalence of chromosomal abnormalities in couples with recurrent miscarriage. Fertil. Steril. *88*, 721–723.
17. Martinelli, I., Ruggenenti, P., Cetin, I., Pardi, G., Perna, A., Vergani, P., Acaia, B., Facchinetti, F., La Sala, G.B., Bozzo, M., et al.; HAPPY Study Group (2012). Heparin in pregnant women with previous placenta-mediated pregnancy complications: a prospective, randomized, multicenter, controlled clinical trial. Blood *119*, 3269–3275.
18. Casals-Casas, C., and Desvergne, B. (2011). Endocrine disruptors: from endocrine to metabolic disruption. Annu. Rev. Physiol. *73*, 135–162.
19. Giakoumelou, S., Wheelhouse, N., Cuschieri, K., Entrican, G., Howie, S.E., and Horne, A.W. (2016). The role of infection in miscarriage. Hum. Reprod. Update *22*, 116–133.
20. Yougbaré, I., Tai, W.S., Zdravic, D., Oswald, B.E., Lang, S., Zhu, G., Leong-Poi, H., Qu, D., Yu, L., Dunk, C., et al. (2017). Activated NK cells cause placental dysfunction and miscarriages in fetal alloimmune thrombocytopenia. Nat. Commun. *8*, 224.
21. Garzia, E., Clauser, R., Persani, L., Borgato, S., Bulfamante, G., Avagliano, L., Quadrelli, F., and Marconi, A.M. (2013). Prolactin and proinflammatory cytokine expression at the fetomaternal interface in first trimester miscarriage. Fertil. Steril. *100*, 108–115 e1–2.
22. Sonalkar, S., Ogden, S.N., Tran, L.K., and Chen, A.Y. (2017). Comparison of complications associated with induction by misoprostol versus dilation and evacuation for second-trimester abortion. Int. J. Gynaecol. Obstet. *138*, 272–275.
23. Xu, B., Zhang, J., Xu, Y., Lu, J., Xu, M., Chen, Y., Bi, Y., and Ning, G. (2013). Association between history of abortion and metabolic syndrome in middle-aged and elderly Chinese women. Front. Med. *7*, 132–137.
24. Yang, B., Zhang, L., Cao, Y., Chen, S., Cao, J., Wu, D., Chen, J., Xiong, H., Pan, Z., Qiu, F., et al. (2017). Overexpression of lncRNA IGFBP4-1 reprograms energy metabolism to promote lung cancer progression. Mol. Cancer *16*, 154.
25. Xiao, Z.D., Han, L., Lee, H., Zhuang, L., Zhang, Y., Baddour, J., Nagrath, D., Wood, C.G., Gu, J., Wu, X., et al. (2017). Energy stress-induced lncRNA FILNC1 represses c-Myc-mediated energy metabolism and inhibits renal tumor development. Nat. Commun. *8*, 783.
26. Liao, M., Liao, W., Xu, N., Li, B., Liu, F., Zhang, S., Wang, Y., Wang, S., Zhu, Y., Chen, D., et al. (2019). LncRNA EPB41L4A-AS1 regulates glycolysis and glutaminolysis by mediating nucleolar translocation of HDAC2. EBioMedicine *41*, 200–213.

27. Yabuta, N., Onda, H., Watanabe, M., Yoshioka, N., Nagamori, I., Funatsu, T., Toji, S., Tamai, K., and Nojima, H. (2006). Isolation and characterization of the TIGA genes, whose transcripts are induced by growth arrest. Nucleic Acids Res. *34*, 4878–4892.

28. Vander Heiden, M.G., Cantley, L.C., and Thompson, C.B. (2009). Understanding the Warburg effect: the metabolic requirements of cell proliferation. Science *324*, 1029–1033.

29. Deblois, G., St-Pierre, J., and Giguère, V. (2013). The PGC-1/ERR signaling axis in cancer. Oncogene *32*, 3483–3490.

30. Taherzadeh-Fard, E., Saft, C., Akkad, D.A., Wieczorek, S., Haghikia, A., Chan, A., Epplen, J.T., and Arning, L. (2011). PGC-1alpha downstream transcription factors NRF-1 and TFAM are genetic modifiers of Huntington disease. Mol. Neurodegener. *6*, 32.

31. Wende, A.R., Huss, J.M., Schaeffer, P.J., Giguère, V., and Kelly, D.P. (2005). PGC-1alpha coactivates PDK4 gene expression via the orphan nuclear receptor ERRalpha: a mechanism for transcriptional control of muscle glucose metabolism. Mol. Cell. Biol. *25*, 10684–10694.

32. Nakagawa, S., Shimada, M., Yanaka, K., Mito, M., Arai, T., Takahashi, E., Fujita, Y., Fujimori, T., Standaert, L., Marine, J.C., and Hirose, T. (2014). The lncRNA Neat1 is required for corpus luteum formation and the establishment of pregnancy in a subpopulation of mice. Development *141*, 4618–4627.

33. Xu, S., Wang, P., You, Z., Meng, H., Mu, G., Bai, X., Zhang, G., Zhang, J., and Pang, D. (2016). The long non-coding RNA EPB41L4A-AS2 inhibits tumor proliferation and is associated with favorable prognoses in breast cancer and other solid tumors. Oncotarget *7*, 20704–20717.

34. Kingdom, J.C., and Kaufmann, P. (1997). Oxygen and placental villous development: origins of fetal hypoxia. Placenta *18*, 613–621, discussion 623–626.

35. Burton, G.J., Jauniaux, E., and Murray, A.J. (2017). Oxygen and placental development; parallels and differences with tumour biology. Placenta *56*, 14–18.

36. McCommis, K.S., and Baines, C.P. (2012). The role of VDAC in cell death: friend or foe? Biochim. Biophys. Acta *1818*, 1444–1450.

37. Shoshan-Barmatz, V., Mizrachi, D., and Keinan, N. (2013). Oligomerization of the mitochondrial protein VDAC1: from structure to function and cancer therapy. Prog. Mol. Biol. Transl. Sci. *117*, 303–334.

38. Magrì, A., Reina, S., and De Pinto, V. (2018). VDAC1 as Pharmacological Target in Cancer and Neurodegeneration: Focus on Its Role in Apoptosis. Front Chem. *6*, 108.

39. Shoshan-Barmatz, V., De Pinto, V., Zweckstetter, M., Raviv, Z., Keinan, N., and Arbel, N. (2010). VDAC, a multi-functional mitochondrial protein regulating cell life and death. Mol. Aspects Med. *31*, 227–285.

40. Semba, H., Takeda, N., Isagawa, T., Sugiura, Y., Honda, K., Wake, M., Miyazawa, H., Yamaguchi, Y., Miura, M., Jenkins, D.M., et al. (2016). HIF-1α-PDK1 axis-induced active glycolysis plays an essential role in macrophage migratory capacity. Nat. Commun. *7*, 11635.

41. Kim, J.W., Tchernyshyov, I., Semenza, G.L., and Dang, C.V. (2006). HIF-1-mediated expression of pyruvate dehydrogenase kinase: a metabolic switch required for cellular adaptation to hypoxia. Cell Metab. *3*, 177–185.

42. Semenza, G.L. (2010). HIF-1: upstream and downstream of cancer metabolism. Curr. Opin. Genet. Dev. *20*, 51–56.

43. Grandjean, G., de Jong, P.R., James, B., Koh, M.Y., Lemos, R., Kingston, J., Aleshin, A., Bankston, L.A., Miller, C.P., Cho, E.J., et al. (2016). Definition of a Novel Feed-Forward Mechanism for Glycolysis-HIF1α Signaling in Hypoxic Tumors Highlights Aldolase A as a Therapeutic Target. Cancer Res. *76*, 4259–4269.

44. Peek, C.B., Levine, D.C., Cedernaes, J., Taguchi, A., Kobayashi, Y., Tsai, S.J., Bonar, N.A., McNulty, M.R., Ramsey, K.M., and Bass, J. (2017). Circadian Clock Interaction with HIF1α Mediates Oxygenic Metabolism and Anaerobic Glycolysis in Skeletal Muscle. Cell Metab. *25*, 86–92.

45. Xiang, S., Gu, H., Jin, L., Thorne, R.F., Zhang, X.D., and Wu, M. (2018). LncRNA IDH1-AS1 links the functions of c-Myc and HIF1α via IDH1 to regulate the Warburg effect. Proc. Natl. Acad. Sci. USA *115*, E1465–E1474.

46. Thrash-Bingham, C.A., and Tartof, K.D. (1999). aHIF: a natural antisense transcript overexpressed in human renal cancer and during hypoxia. J. Natl. Cancer Inst. *91*, 143–151.